



Stimulated Brillouin scattering of terahertz electromagnetic pulses in paraelectrics

V. Grimalsky¹ · S. Koshevaya¹ · J. Escobedo-Alatorre¹ · E. Jatirian-Foltides¹

Received: 4 May 2018 / Accepted: 16 December 2018 / Published online: 2 January 2019
© Springer-Verlag GmbH Germany, part of Springer Nature 2019

Abstract

The nonlinear acoustoelectromagnetic phenomena in the terahertz (THz) range in the crystalline paraelectric SrTiO₃ are investigated theoretically. The goal is to investigate an appearance of short THz electromagnetic (EM) pulses. The moderate cooling to the temperature $T \approx 77$ K is considered. The resonant three-wave interaction of two counterpropagating EM THz waves with the longitudinal acoustic wave of the difference frequency is under investigation that is called the stimulated Brillouin scattering. This resonant interaction is due to the quadratic nonlinearity called electrostriction. The appearance of short EM pulses is possible when the input amplitudes of the signal EM wave are comparable with the pump amplitude and the duration of the input pulses is quite long. In the temporal scale associated with the EM wave propagation within a crystal, the cubic EM nonlinearity and the EM wave dispersion affect this three-wave resonant interaction. Under the development of the resonant nonlinear interaction, the modulation instability occurs that results in the complex and even chaotic wave modulation.

1 Introduction

Now, the assimilation of the terahertz (THz) range 0.1–30 THz occurs [1, 2]. An important problem is creating short electromagnetic (EM) pulses of THz range, both baseband and envelope ones. For this purpose, it is possible to use the joint action of EM cubic nonlinearity and the frequency dispersion of certain signs to realize the modulation instability of long input pulses and the propagation of envelope solitons [3–7]. Also, the short envelope EM pulses can be formed under three-wave resonant interaction of two counterpropagating EM waves with an acoustic wave or a space charge wave of the difference frequency, the so-called stimulated Brillouin scattering (SBS) [8–10]. In nonlinear dielectrics, SBS is due to the quadratic nonlinearity called the electrostriction.

The nonlinear dielectrics, semiconductors, and semi-metals can be used as volume nonlinear materials in terahertz (THz) range [1, 2]. The ferroelectrics in the non-polar phase are utilized as the nonlinear dielectrics, the so-called

paraelectrics like SrTiO₃, KTaO₃, and ceramics on their base [11–31]. The crystalline SrTiO₃ possesses high cubic EM nonlinearity and relatively low losses in the lower part of THz range 0.1–1 THz at moderately low temperatures $T = 50$ – 90 K. In a distinction from the microwave range, there exists the frequency dispersion in THz range when the EM frequency is close to the soft mode frequency, i.e., the lowest frequency of oscillations of the optical type of the crystalline lattice. In the crystalline SrTiO₃, the soft mode frequency decreases with the decrease of the temperature. The modulation instability of long input EM envelope and baseband pulses takes place due to the joint action of the cubic nonlinearity and the frequency dispersion [6, 7, 32]. Also, the resonant three-wave nonlinear interaction between counterpropagating EM waves and the acoustic wave occurs due to the electrostriction, the so-called stimulated Brillouin scattering (SBS) [17–21, 23]. The electrostriction moduli are also high in SrTiO₃. Generally, the joint action of the quadratic electrostriction nonlinearity, the cubic EM nonlinearity, the EM frequency dispersion, and EM dissipation takes place under SBS [4, 8, 33].

In this paper, SBS of EM THz waves is under investigation, see Fig. 1. The three-wave resonant interaction occurs between two counterpropagating transverse EM waves of the circular frequencies ω_1 , ω_2 and the wave numbers k_1 , k_2 with

✉ V. Grimalsky
v_grim@yahoo.com; svetlana@uaem.mx

¹ CIICAp, IICBA, Autonomous University of State Morelos (UAEM), Av. Universidad 1001, 62209 Cuernavaca, Morelos, Mexico

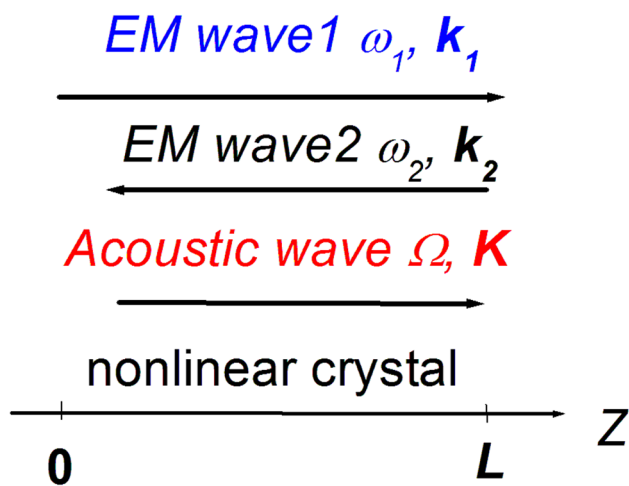


Fig. 1 The geometry of the problem. The nonlinear crystal occupies the region $0 < z < L$. At the boundaries, the matched loads are assumed to prevent the reflection of EM waves. In the transverse directions x, y , the system is uniform

the longitudinal acoustic wave with the circular frequency and the wave number Ω, K .

The resonant matching conditions are

$$\begin{aligned} \omega_1 &= \omega_2 + \Omega, & k_1 &= -|k_2| + K; & k_1 &= \frac{\omega_1}{c}(\epsilon'(\omega_1))^{1/2} \\ |k_2| &= \frac{\omega_2}{c}(\epsilon'(\omega_2))^{1/2} \approx k_1, & K &= \frac{\Omega}{s} \approx 2k_1, \end{aligned} \tag{1}$$

Here $\epsilon'(\omega)$ is the real part of the linear dielectric permittivity of SrTiO₃, s is the velocity of the longitudinal acoustic wave. The pump EM wave at the frequency ω_1 and the wave number k_1 is a continuous wave that propagates from $z=0$ to $z=L$. Also, a short signal pulse of EM wave at the frequency $\omega_2 < \omega_1$ and the wave number $k_2 < 0$ is input at $z=L$ and propagates to $z=0$. It is demonstrated that the resonant interaction results in the amplification of EM pulses at the frequency ω_2 , and several short envelope signal pulses of high peak amplitudes are generated within the crystal. The EM cubic nonlinearity, the frequency dispersion, and the EM wave dissipation affect essentially the nonlinear wave interaction. The input signal amplitudes should be chosen quite high compared with the input pump amplitudes to provide the pulse compression at the output of the crystal.

2 Basic equations

The nonlinear propagation and interaction of transverse EM waves with the electric field component $E_x = E$ is considered along OZ axis within the crystalline paraelectric SrTiO₃. EM waves can interact with the longitudinal acoustic wave of the

mechanic displacement $u = u_z$. The cubic EM nonlinearity in the crystalline SrTiO₃ is due to the nonlinear properties of the lattice polarization $\epsilon_0 P$, where ϵ_0 is the electric constant in SI units. In the one-dimensional case, the basic equations that describe the nonlinear EM wave propagation and the nonlinear interaction with the longitudinal acoustic wave in the paraelectric crystalline SrTiO₃ are [7, 14, 15, 23]:

$$\begin{aligned} \frac{\partial^2 P}{\partial t^2} + \gamma \frac{\partial P}{\partial t} + \omega_T^2 \left(1 + \frac{P^2}{P_0^2} \right) P &= \epsilon(0)\omega_T^2 E; \\ \frac{\partial^2 E}{\partial z^2} &= \frac{1}{c^2} \frac{\partial^2 P}{\partial t^2} + \frac{a}{c^2} \frac{\partial^2}{\partial t^2} \left(\frac{\partial u}{\partial z} E \right); \\ \rho \frac{\partial^2 u}{\partial t^2} &= \frac{\partial \sigma}{\partial z}; \end{aligned}$$

where $D \equiv \epsilon_0 \left(E + P + a \frac{\partial u}{\partial z} E \right) \approx \epsilon_0 \left(P + a \frac{\partial u}{\partial z} E \right)$;

$$\sigma \equiv \rho s^2 \frac{\partial u}{\partial z} + \rho \nu \frac{\partial^2 u}{\partial z \partial t} - \frac{\epsilon_0 a}{2} E^2. \tag{2}$$

Here $D \equiv D_x$ is the electric induction, $\sigma \equiv \sigma_{zz}$ is the mechanic stress, ω_T is the soft mode frequency, which is in the lower part of THz range for SrTiO₃, γ is the lattice EM dissipation; $\rho \approx 5 \text{ g/cm}^3$ is the mass density, $s \approx 8 \times 10^5 \text{ cm/s}$ is the velocity of the longitudinal acoustic wave, a is the electrostriction module, $\rho \nu$ is the acoustic dissipation due to viscosity. At the temperature $T \approx 77 \text{ K}$, it is $\omega_T \approx 6 \cdot 10^{12} \text{ s}^{-1}$, $\gamma = 2 \times 10^{11} \text{ s}^{-1}$, and the static linear dielectric permittivity is $\epsilon(0) \equiv \epsilon(\omega = 0) = 1.8 \times 10^3$. In SrTiO₃ the permittivity increases with the decrease of temperature, whereas the lattice dissipation γ possesses the minimum at $T \approx 77 \text{ K}$.

In Eq. (2), the cubic EM nonlinearity, i.e., the term with $(P/P_0)^2 P$, is determined by the parameter P_0 . This parameter is related to the characteristic magnitude of the electric field E_0 where the cubic EM nonlinearity is essential, namely $P_0 = \epsilon(0)E_0$. At the temperature $T \approx 77 \text{ K}$, it is $E_0 = 60 \text{ kV/cm}$ [7, 14, 15]. The estimation of the electrostriction module is $a \approx -\epsilon(0)^2/5$ [23], whereas the cubic nonlinearity is proportional to $\epsilon(0)^3$. Because of the small EM dissipation in the crystalline SrTiO₃, the nonlinearity manifests at the amplitudes of EM waves at least one order smaller than E_0 .

Here the dynamics of SBS is considered, where two counterpropagating envelope EM waves interact with the longitudinal acoustic wave of the difference frequency. The electric field of EM waves and the longitudinal acoustic displacement are represented as:

$$\begin{aligned} E &= \frac{1}{2} A_1(z, t) e^{i\omega_1 t - ik_1 z} + \frac{1}{2} A_2(z, t) e^{i\omega_2 t + i|k_2|z} + \text{c.c.} \\ u &= \frac{1}{2} U(z, t) e^{i\Omega t - iKz} + \text{c.c.}; \end{aligned} \tag{3}$$

In Eq. (3) $A_{1,2}$ are slowly varying amplitudes for the pump and signal EM waves, U is the corresponding amplitude of the acoustic wave. The resonant matching conditions between the frequencies $\omega_{1,2}$, Ω and the wave numbers $k_{1,2}$, K are given in Eq. (1).

From Eq. (2), the following well-known expression for the linear dielectric permittivity can be achieved:

$$\epsilon(\omega) \approx \frac{\epsilon(\omega = 0) \cdot \omega_T^2}{\omega_T^2 - \omega^2 + i\gamma\omega}, \quad \omega > 0. \tag{4}$$

Thus, the linear dispersion equation for EM waves is

$$\omega(k) = ck \cdot \left(\epsilon(0) + \frac{c^2 k^2}{\omega_T^2} \right)^{-1/2}. \tag{5}$$

It is used to calculate the group velocity and the wave dispersion.

The coupled equations for the slowly varying amplitudes have been derived [3–9, 32–36]:

$$\begin{aligned} & \frac{\partial A_1}{\partial t} + v_g \frac{\partial A_1}{\partial z} + ig \frac{\partial^2 A_1}{\partial z^2} + \Gamma_e A_1 \\ & + iN \cdot (|A_1|^2 + 2|A_2|^2)A_1 = -\alpha_1 A_2 U; \\ & \frac{\partial A_2}{\partial t} - v_g \frac{\partial A_2}{\partial z} + ig \frac{\partial^2 A_2}{\partial z^2} + \Gamma_e A_2 \\ & + iN \cdot (2|A_1|^2 + |A_2|^2)A_2 = \alpha_1 A_1 U^*; \\ & \frac{\partial U}{\partial t} - \frac{i}{2\Omega} \frac{\partial^2 U}{\partial t^2} + \Gamma_a U = \alpha_a A_1 A_2^*. \end{aligned} \tag{6}$$

The following expressions are used for the coefficients:

$$\begin{aligned} \alpha_1 &= \frac{a\omega_1^2 v_g}{2c^2}, \quad \alpha_a = \frac{a\epsilon_0}{4\rho s}, \quad v_g \equiv \left. \frac{\partial \omega(k)}{\partial k} \right|_{\omega=\omega_1} > 0, \\ g &= \frac{1}{2} \left. \frac{\partial^2 \omega(k)}{\partial k^2} \right|_{\omega=\omega_1} < 0, \\ \Gamma_e &= \frac{\omega_1^2}{2\omega_T^2} \gamma, \quad \Gamma_a = \frac{\nu}{2} K^2, \quad N = -\frac{3\omega_1}{8E_0^2 \left(1 - \frac{\omega_1^2}{\omega_T^2}\right)^2} < 0. \end{aligned}$$

Here v_g is the EM wave group velocity, g is the EM wave dispersion coefficient, Γ_e , Γ_a are the EM and acoustic dissipation coefficients, respectively, N is the coefficient of the EM cubic nonlinearity. It is assumed that the following parameters are small: $(\omega_1 t_n)^{-1} \ll 1$, $(k_1 l_n)^{-1} \ll 1$, where $l_n \geq 10 \mu\text{m}$ is the characteristic spatial scale, $t_n = l_n/v_g$ is the temporal one.

The terms with EM cubic nonlinearity and EM wave dispersion have been taken from [7], where the method of

deriving the equations for slowly varying amplitudes and then the modulation instability of EM pulses were investigated in detail. The three-wave interaction occurs in the temporal scale related to the propagation of EM waves within the crystal with the group velocity $v_g \approx c/\epsilon(0)^{1/2} \gg s$, so the convective term for the acoustic waves $s(\partial U/\partial z)$ is small. But, it is necessary to preserve the term with the second derivative with respect to time $\partial^2 U/\partial t^2$, because the characteristic temporal scale is $t_n = 10\text{--}100 \text{ ps}$ and thus $t_n \Omega \sim 1$. The analogous situation occurs for SBS in optical fibers, but only when the extreme compression of optical pulses takes place there [37].

The boundary conditions for EM waves are:

$$A_1(z = 0, t) = A_{10} \tanh\left(\frac{t}{t_{01}}\right), \quad A_2(z = L, t) = A_{20} e^{-\left(\frac{t-t_1}{t_{02}}\right)^2}. \tag{7}$$

The amplitude of the input pump wave A_1 is constant after a short transition time $t_{01} \ll t_1$, whereas the input signal wave A_2 is pulse-like of a duration t_{02} . The acoustic wave is excited during the nonlinear resonant interaction. The reflections of EM waves at the boundaries are assumed absent due to the perfect matching.

The input amplitudes A_{10} , A_{20} are chosen below the threshold for the modulation instability. The used frequencies are $\omega_1 = 1.5 \times 10^{12}\text{--}4 \times 10^{12} \text{ s}^{-1} \approx \omega_2$, $\Omega \approx 5 \times 10^9\text{--}1 \times 10^{10} \text{ s}^{-1}$. The results of simulations are tolerant to changes of used parameters. At higher pump frequencies ω_1 the EM wave dissipation coefficient Γ_e is very high, whereas at smaller frequencies the generation of the third EM harmonic becomes important [22]. The generation of higher harmonics is a parasitic process there. The length of the crystal is $L = 0.005\text{--}0.015 \text{ cm}$. The acoustic dissipation coefficient is $\Gamma_a = 5 \times 10^5\text{--}2 \times 10^6 \text{ s}^{-1}$.

The approximation of finite differences has been used in simulations of Eq. (6). The unconditionally stable implicit difference schemes have been applied for A_1 , A_2 [38]. The equation for the acoustic amplitude U has been approximated by the explicit scheme:

$$\begin{aligned} & \frac{\partial U}{\partial t} - \frac{i}{2\Omega} \frac{\partial^2 U}{\partial t^2} + \Gamma_a U \approx \frac{U^{p+1} - U^{p-1}}{2\tau} - \frac{i}{2\Omega} \frac{U^{p+1} - 2U^p + U^{p-1}}{\tau^2} \\ & + \Gamma_a \frac{U^{p+1} + U^{p-1}}{2} = \alpha_a (A_1 A_2^*)^p. \end{aligned} \tag{8}$$

Here τ is the temporal step, $U^p \equiv U(p\tau)$. The temporal step should be chosen quite small to provide the numerical stability. Using implicit schemes for U yields the same results, but occupies more time.

3 Results of numerical simulations

The main goal of the simulations is the possibility to obtain short EM pulses at the signal frequency under SBS at the output $z=0$. The amplitudes of EM waves are related to $E_0=60$ kV/cm. The acoustic displacement is related to the elastic deformation $K|U_0|=10^{-4}$. For all simulations, the input amplitude A_{10} of the pump EM wave has been chosen below the threshold of the modulation instability due to the cubic nonlinearity [7, 28].

The typical results of simulations are presented in Figs. 2, 3, 4, 5 and 6. For all the cases, the pump frequency is $\omega_1=3 \times 10^{12} \text{ s}^{-1} \approx \omega_2$, the acoustic frequency is $\Omega \approx 8 \times 10^9 \text{ s}^{-1}$. The acoustic dissipation coefficient is $\Gamma_a=10^6 \times \text{s}^{-1}$.

In Fig. 2, the pump and signal EM waves at the output are presented for different lengths of the crystal. One can see that there exists the optimum length where the formation of several compressed amplified EM signal pulses at the frequency ω_2 occurs at the output $z=0$. Under used parameters, it is $L=0.007$ cm $\equiv 70$ μm . At bigger or smaller lengths, the maximum values of the signal pulses at the output are smaller than ones at this optimum length. Thus, in Figs. 4, 5 and 6 namely this length is used, but the maximum amplitude A_{20} and the duration t_{02} of the input signal vary.

Several amplified compressed pulses of the signal EM wave are formed at $z=0$ when the amplitudes of the input signal exceed some value. Also, the durations of the input signal pulses should be large enough. This can be explained by an essential influence of the cubic EM nonlinearity and EM wave dispersion on the resonant three-wave interaction. The joint action of the cubic nonlinearity and the EM wave dispersion prevents forming three-wave solitons that can propagate in the case of the pure three-wave nonlinear interaction [33] and can be realized experimentally in optical fibers. In another words, in nonlinear paraelectric crystals, there exists a competition between the three-wave resonant nonlinear interaction due to the quadratic nonlinearity and the formation of envelope solitons due to the cubic nonlinearity and the EM wave dispersion.

The durations of the output signal pulses are of about 10 ps, see Fig. 2e, f, so the EM compression is not limited by the period of the acoustic wave $2\pi/\Omega \sim 5 \times 10^{-10} \text{ s} \equiv 500$ ps. This is similar to the behavior of compressed pulses in optical fibers in the optical range [37], but the spatial and temporal scales are different from the case of THz range in SrTiO₃ crystals.

From a comparison of Figs. 2, 4, 5 and 6, it is possible to conclude that the shortening of the input signal pulses down till 50–20 ps can prevent the excitation of the compressed signal pulses at the output, even when the input signal amplitudes are quite high.

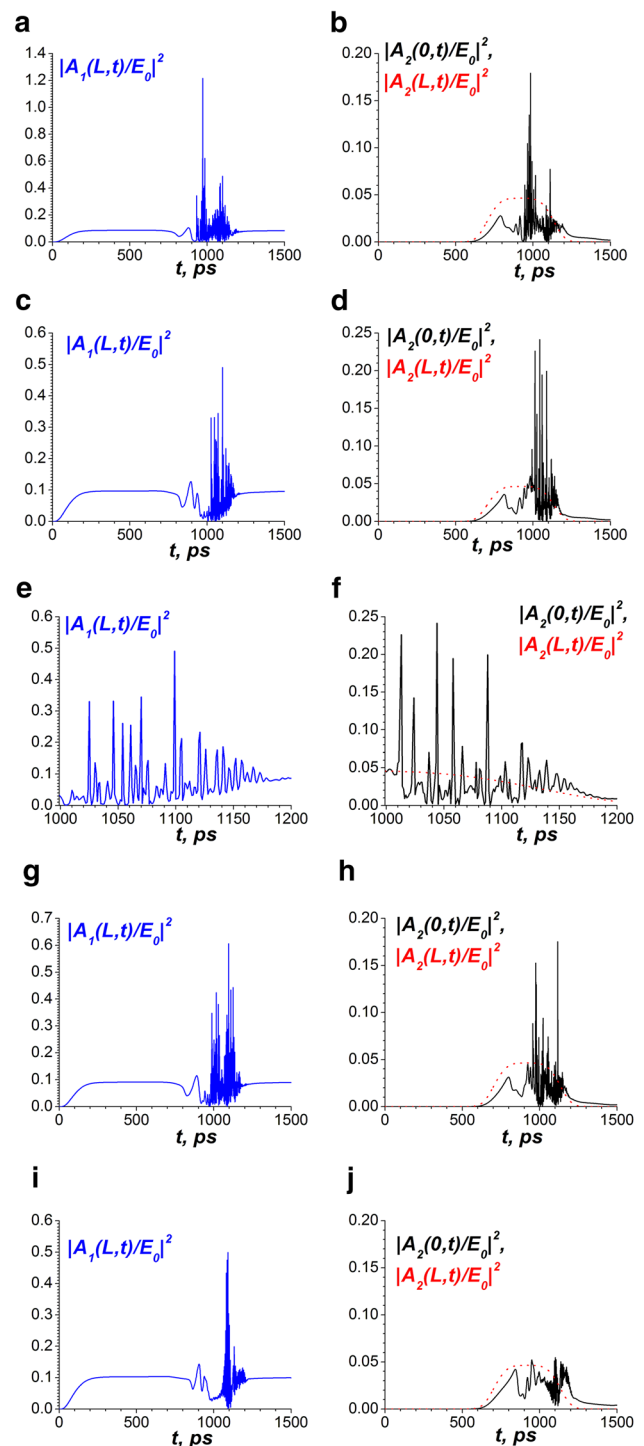


Fig. 2 The dynamics of SBS. Left panels are the output amplitudes $|A_1(z=L,t)/E_0|^2$ of the pump wave at the frequency ω_1 . Right panels are the input amplitudes $|A_2(z=L,t)/E_0|^2$ and output ones $|A_2(z=0,t)/E_0|^2$ of the signal wave at the frequency ω_2 . The input signal pulse $|A_2(z=L,t)/E_0|^2$ is given by the dot lines there. The parameters are $A_{10}=25.9$ kV/cm, $A_{20}=12.9$ kV/cm ($A_{10}/E_0=0.43$, $A_{10}/E_0=0.215$), $t_1=1$ ns, $t_{02}=300$ ps. **a, b** are for the length of the crystal $L=0.008$ cm $\equiv 80$ μm ; **c–f** are for the length of the crystal $L=0.007$ cm $\equiv 70$ μm ; **e, f** are detailed views; **g, h** are for the length of the crystal $L=0.0075$ cm $\equiv 75$ μm ; **i, j** are for the length of the crystal $L=0.0065$ cm $\equiv 65$ μm

Fig. 3 The spatial profiles of the interacting waves; **a–c** are for the time moments $t=900$, 1000, 1100 ps. The length of the crystal is $L=0.007$ cm \equiv 70 μ m, see Fig. 2c–f. The amplitudes $|A_1|^2$ are given by solid lines, $|A_2|^2$, $|U|^2$ are given by dash and dot lines, correspondingly

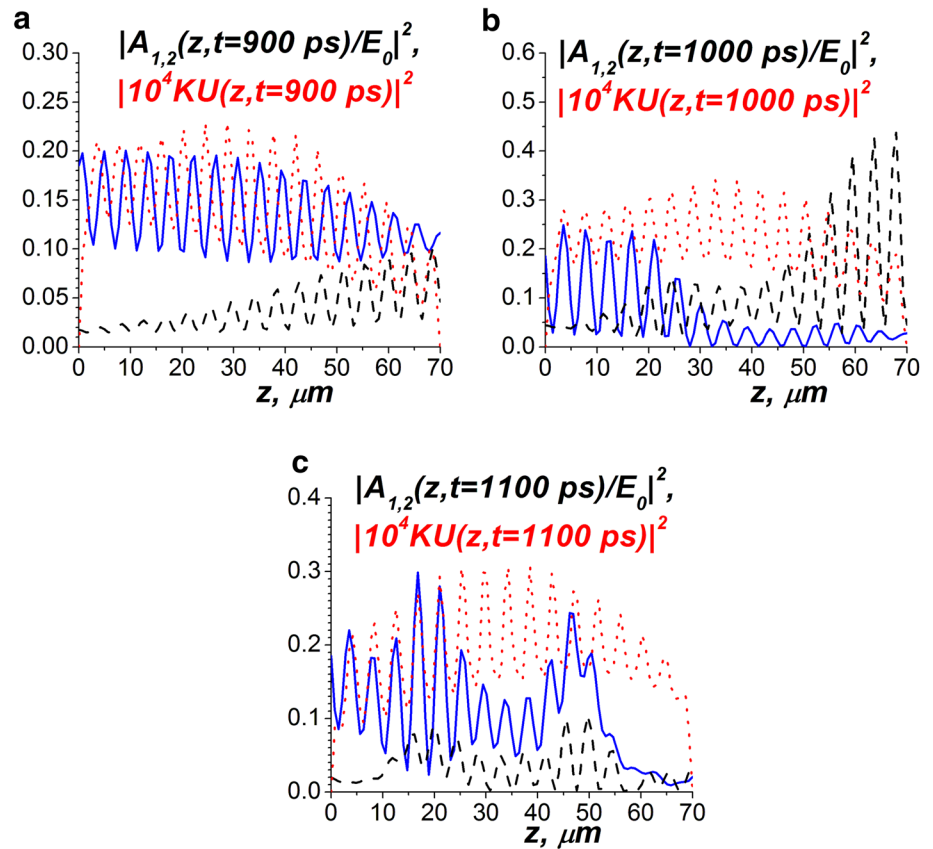


Fig. 4 The dynamics of SBS. Left panels are the output amplitude $|A_1(z=L,t)/E_0|^2$ of the wave at the frequency ω_1 . Right panels are the input amplitudes $|A_2(z=L,t)/E_0|^2$ and output ones $|A_2(z=0,t)/E_0|^2$ of the wave at the frequency ω_2 . The parameters are $A_{10}=25.9$ kV/cm, $A_{20}=18.1$ kV/cm ($A_{10}/E_0=0.43$, $A_{10}/E_0=0.30$); $L=0.007$ cm, $t_1=1$ ns, $t_0=300$ ps. **a, b** are general views, **c, d** are detailed ones

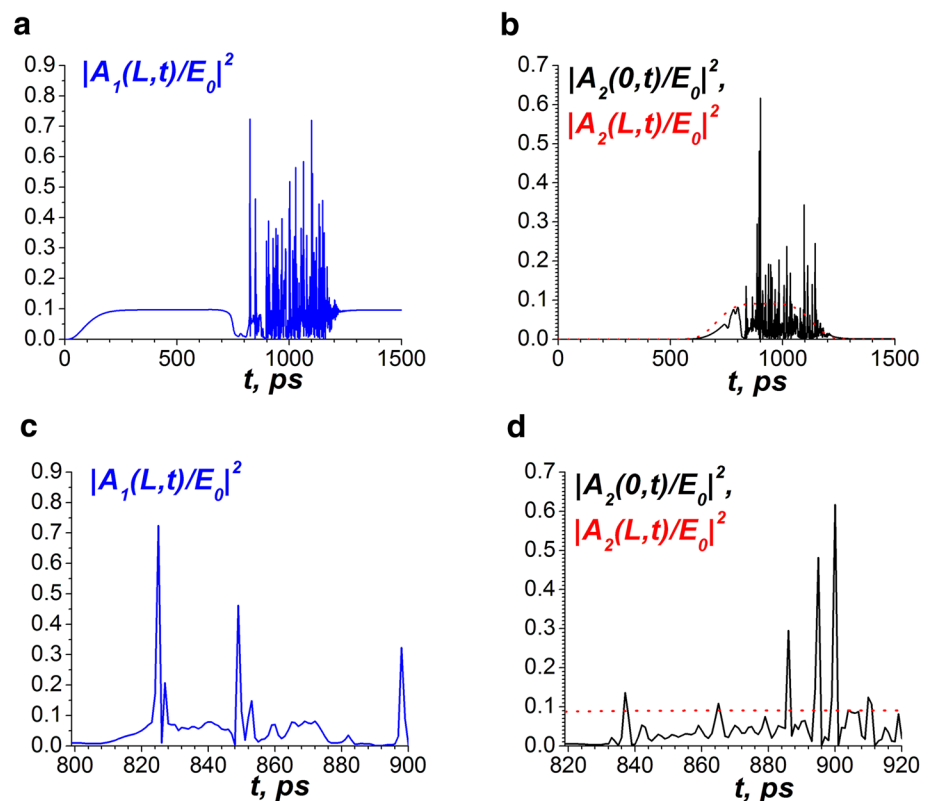


Fig. 5 The same as in Fig. 4, but the parameters are $A_{10}=25.9$ kV/cm, $A_{20}=18.1$ kV/cm, $t_{02}=100$ ps, $L=0.007$ cm. **a, b** are general views, **c, d** are detailed ones

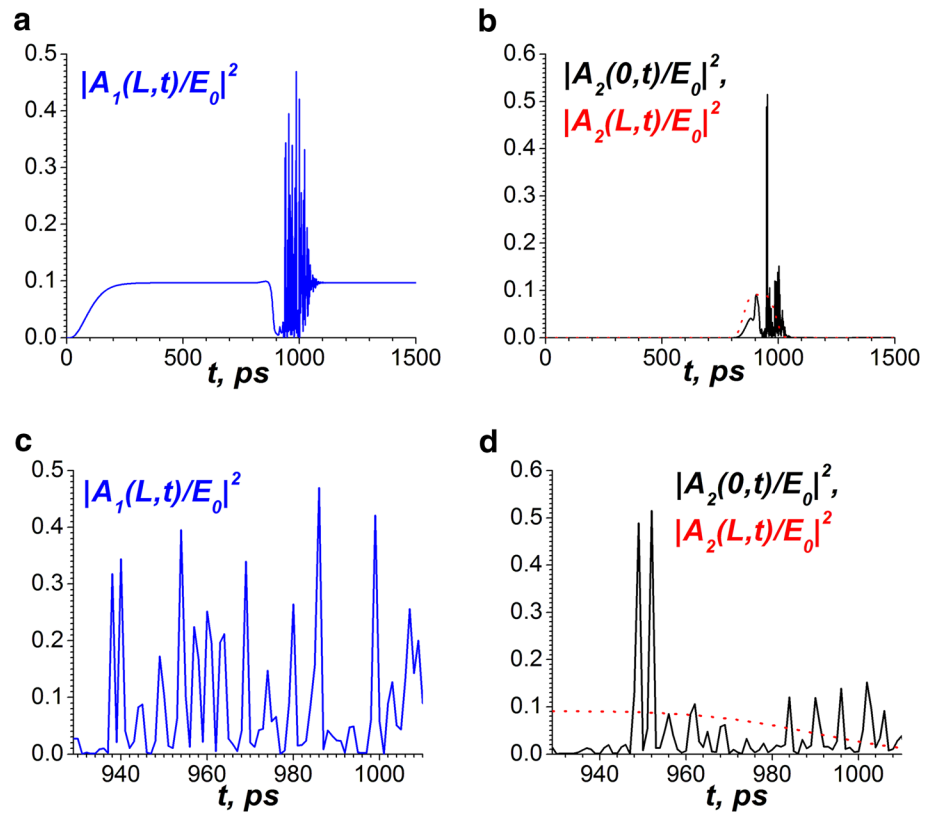


Fig. 6 The same as in Figs. 4, 5, but the parameters are $A_{10}=25.9$ kV/cm, $A_{20}=25.9$ kV/cm ($A_{10}/E_0=0.43$, $A_{10}/E_0=0.43$). $t_{02}=20$ ps; $L=0.007$ cm. **a, b** are general views, **c, d** are detailed ones

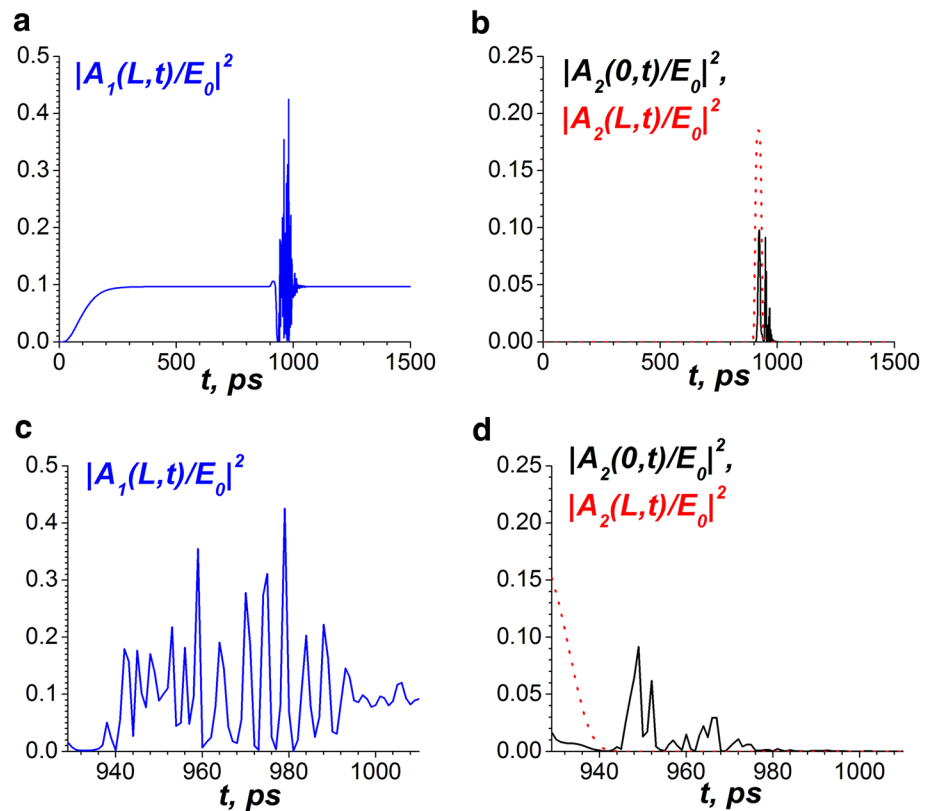
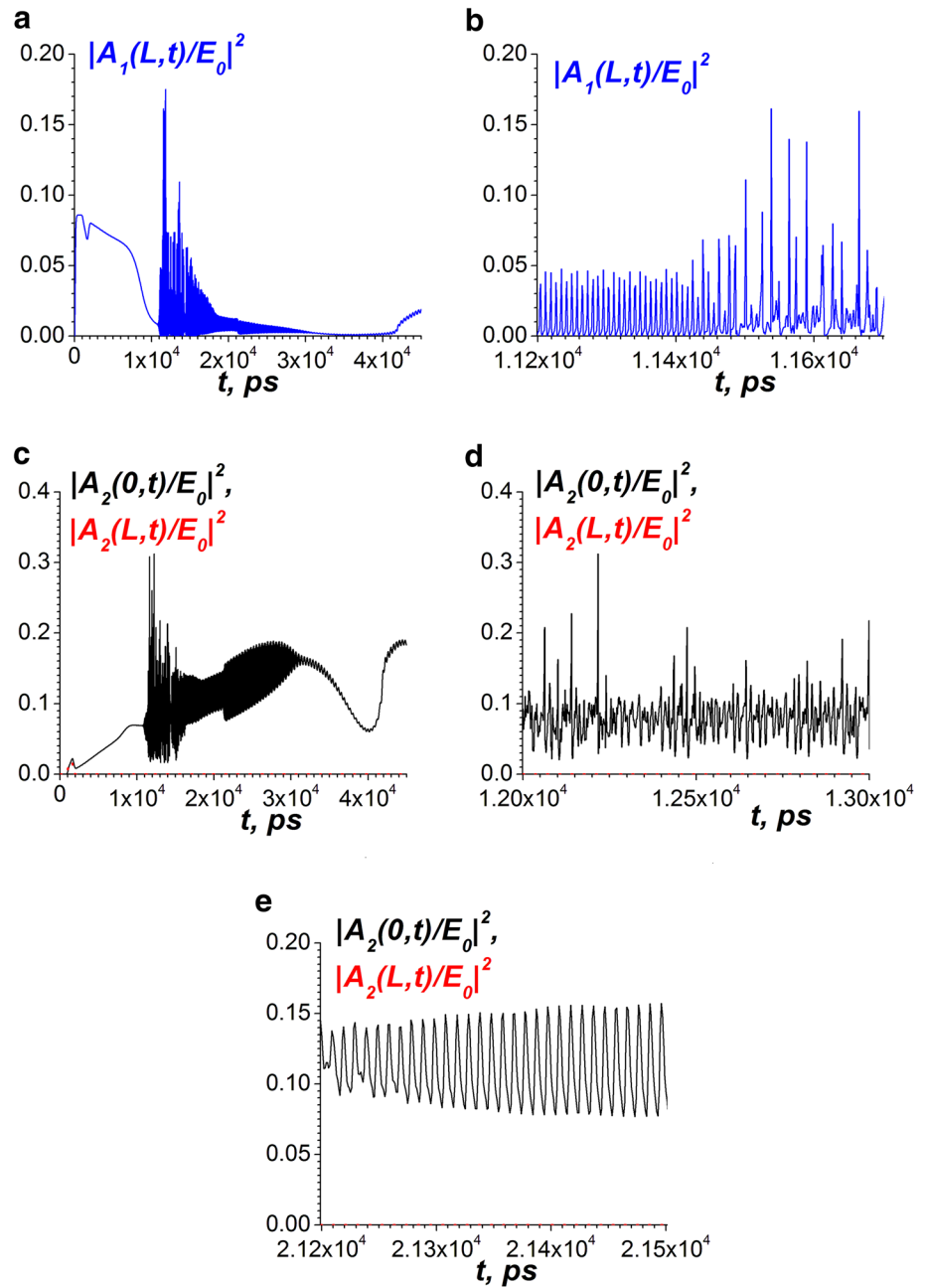


Fig. 7 The dynamics of SBS in the case of a small input signal pulse, $A_{10} = 25.9$ kV/cm, $A_{20} = 7.44$ kV/cm ($A_{10}/E_0 = 0.43$, $A_{10}/E_0 = 0.125$). $t_{02} = 500$ ps. The length of the crystal is $L = 0.008$ cm. **a, c** are general views, **b, d, e** are detailed ones



Because the signal EM wave propagates oppositely to the pump EM wave and the acoustic wave practically does not move within the temporal scale of the interaction and accumulates within the system, the parametric nonlinear resonator forms within the crystal [39]. As a result, after some time $t \sim 10\text{--}20$ ns $\gg t_n \approx 10$ ps, this leads to the continuous excitation of the signal EM wave ω_2 , and the modulation instability due to the mutual influence of EM waves occurs due to the cubic nonlinearity and EM wave dispersion. Note that in Eq. (6), the mutual influence of EM waves due to the cubic nonlinearity is two times bigger than the self-action. The dynamics becomes irregular and even chaotic, as seen

in Fig. 7 at the times $t > 10$ ns. The nonlinear wave dynamics seems complex there, sometimes the intermittency between chaotic and regular regimes of auto oscillations occurs.

4 Conclusions

The resonant three-wave interaction of two counterpropagating terahertz electromagnetic waves at the frequencies $\omega_{1,2}$ with the longitudinal acoustic wave of the different frequencies can be realized in the paraelectric crystals like SrTiO₃ in the lower frequency part of the terahertz range at frequencies

$f_1 \approx f_2 = 0.3\text{--}0.7$ THz, or $\omega = 2\pi f = 2 \times 10^{12}\text{--}4 \times 10^{12}$ s⁻¹, below the soft mode frequency $f_T \approx 1$ THz. The moderate cooling $T \approx 77$ K should be used. This interaction is due to the quadratic nonlinearity called electrostriction and is analogous to the stimulated Brillouin scattering in optics. The resonant nonlinear interaction can be used for the generation of several short amplified electromagnetic pulses at the signal frequency f_2 . The input amplitudes and durations of the amplified signal wave pulses should be bigger than certain values; this can be explained by an essential influence of the cubic electromagnetic nonlinearity and the electromagnetic wave dispersion on this three-wave resonant interaction. It is important that the electromagnetic pulse compression is not limited by the period of the resonant acoustic wave.

Because the velocity of the acoustic wave is several orders smaller than the electromagnetic wave velocity, the acoustic energy accumulates within the nonlinear crystal. Thus, the bounded crystal behaves as an electromagnetic resonator even without the reflection of electromagnetic waves at the boundaries. This can lead to complex regimes of this three-wave resonant interaction like the modulation instability of electromagnetic waves of either chaotic or regular character.

Acknowledgements The authors thank SEP-CONACyT, Mexico, for partial support of this work.

References

1. Yun-Shik, Lee, *Principles of Terahertz Science and Technology* (Springer, New York, 2009)
2. M. Perenzoni, D.J. Paul, Eds, *Physics and Applications of Terahertz Radiation* (Springer, New York, 2014)
3. S.A. Akhmanov, V.A. Vysloukh, A.S. Chirkin, *Optics of Femtosecond Laser Pulses* (AIP Publ., New York, 1992)
4. G.P. Agrawal, *Nonlinear Fiber Optics* (Academic Press, New York, 2013)
5. R.W. Boyd, *Nonlinear Optics* (Academic Press, New York, 2013)
6. Y.S. Kivshar, G.P. Agrawal, *Optical Solitons. From Fibers to Photonic Crystals* (Academic Press, New York, 2003)
7. V. Grimalsky, S. Koshevaya, J. Escobedo-Alatorre, M. Tecpoyotl-Torres, J. Electromagn. Anal. Appl. (JEMAA) **8**, 226 (2016). <https://doi.org/10.4236/jemaa.2016.810021>
8. M.J. Damzen, V.I. Vlad, V. Babin, A. Mocofanescu, *Stimulated Brillouin Scattering. Fundamentals and Applications* (IOP Publishing, Bristol, 2003)
9. G. Burlak, S. Koshevaya, E. Gutierrez-D, J. Sanchez-Mondragon, V. Grimalsky, Opt. Quant. Electron. **33**, 661 (2001)
10. V. Grimalsky, S. Koshevaya, G. Burlak, B. Salazar, J. Opt. Soc. Am. B **19**, 689 (2002)
11. I.S. Rez, Yu.M. Poplavko, *Dielectrics. Basic Properties and Applications in Electronics* (Radio and Svyaz', Moscow, 1989) (in Russian)
12. Yu.M. Poplavko, L.P. Pereverzeva, S.O. Voronov, Yu.I. Yaki-menko, *Physical Material Science. Vol. 2. Dielectrics*. (KPI Publishing, Kiev, 2007). ISBN 978-966-622-256-8 (in Ukrainian)
13. S. Gevorgian, *Ferroelectrics in Microwave Devices, Circuits and Systems* (Springer, New York, 2009)
14. O.G. Vendik (ed.), *Ferroelectrics in Microwave Technology* (Sov. Radio, Moscow, 1979) (in Russian)
15. I.V. Ivanov, G.V. Belokopytov, I.M. Buzin, V.M. Sychev, V.F. Chuprakov, Ferroelectrics **21**, 405 (1978). <https://doi.org/10.1080/00150197808237279> (ISSN 00150193)
16. I.V. Ivanov, I.M. Buzin, G.V. Belokopytov, V.M. Sychev, V.F. Chuprakov, Sov. Phys. J. **24**, 684 (1981). <https://doi.org/10.1007/BF00941340> (ISSN 00385697)
17. G.V. Belokopytov, I.V. Ivanov, M.E. Reshetnikov, V.A. Chisty-aev, Pis'ma v Zhurnal Tekhnicheskoy Fiziki (English transl Tech. Phys. Lett.) **10**, 1210 (1984)
18. G.V. Belokopytov: Radiophys. Quantum Electron. **30**, 830 (1987) ISSN: 00338443, <https://doi.org/10.1007/BF01078863>
19. G.V. Belokopytov, V.A. Chistyayev, Radiophys. Quantum Elec-tron. **32**, 123 (1989). <https://doi.org/10.1007/BF01039666> (ISSN 00338443)
20. G.V. Belokopytov, V.N. Semenenko, V.A. Chistyayev, Radiophys. Quantum Electron. **32**, 709 (1989). <https://doi.org/10.1007/BF01060002> (ISSN 00338443)
21. G.V. Belokopytov, Ferroelectrics **167**, 137 (1995). <https://doi.org/10.1080/00150199508232306> (ISSN 00150193)
22. L.G. Gassanov, S.V. Koshevaya, T.N. Narytnik, M.Yu. Omel'yanenko, Izv. VUZ Radioelektron. (English transl Radioelectron. Commun. Syst.) **21**(10), 56 (1978)
23. G.N. Burlak, N.Ya. Kotsarenko, S.V. Koshevaya, Sov. Phys. J. **24**, 732 (1981). <https://doi.org/10.1007/BF00941343> (ISSN 00385697)
24. K. Kamarás, K.L. Barth, F. Keilmann, R. Henn, M. Reedyk, C. Thomsen, M. Cardona, J. Kircher, P.L. Richards, J.L. Stehle, J. Appl. Phys. **78**, 1235 (1995). <https://doi.org/10.1063/1.360364>
25. A. Zamudio-Lara, S.V. Koshevaya, V.V. Grimalsky, F. Yañez-Cortes, Radioelectron. Commun. Syst. **58**, 411 (2015). <https://doi.org/10.3103/S0735272715090034>
26. L.G. Gassanov, S.V. Koshevaya, M.Yu. Omel'yanenko, Radiotekhika Elektron (English transl Radio Eng Electron Phys) **25**, 1238 (1980)
27. S.V. Koshevaya, M.V. Kononov, M.Yu. Omel'yanenko, Izv. VUZ Radioelektron. (English transl Radioelectron. Commun. Syst.) **28**(3), 53 (1985)
28. Yu.G. Rapoport, V.V. Grimalsky, S.V. Koshevaya, D.L. Melendez-Isidoro, *Modulation Instability of Terahertz Electromagnetic Pulses in SrTiO₃ Paraelectric*. Proceedings of the IEEE 35th International Conference on Electronics and Nanotechnology (ELNANO), vol 128, Kyiv, 21–23 April 2015 (2015). <https://doi.org/10.1109/ELNANO.2015.7146851>
29. K.M. Rabe, C.H. Ahn, J.-M. Triscone (eds.), *Physics of Ferroelectrics. A Modern Perspective* (Springer, New York, 2007)
30. M.E. Lines, A.M. Glass, *Principles and Applications of Ferroelectric and Related Materials* (Clarendon Press, Oxford, 1977)
31. B.A. Strukov, A.P. Levanyuk, *Ferroelectric Phenomena in Crystals* (Springer, New York, 1998)
32. M.I. Rabinovich, D.I. Trubetskov, *Oscillations and Waves in Linear and Nonlinear Systems* (Kluwer, Dordrecht, 1989)
33. E. Picholle, C. Montes, IEEE J. Sel. Top. Quantum Electron. **9**, 74 (2003)
34. N. Bloembergen, *Nonlinear Optics* (W.A. Benjamin, Inc., New York, 1965)
35. J. Weiland, H. Wilhelmsson, *Coherent Non-Linear Interaction of Waves in Plasmas* (Pergamon Press, London, 1977)
36. A.P. Sukhorukov, *Nonlinear Wave Interactions in Optics and Radiophysics* (Nauka Publishing, Moscow, 1988) (in Russian)
37. I. Velchev, D. Neshev, W. Hogervorst, W. Ubachs, IEEE J. Quant. Electron. **35**, 3812 (1999)
38. A.A. Samarskii, *Theory of Difference Schemes* (Marcel Dekker, New York, 2001)
39. L.M. Gorbunov, Sov. Phys. Tech. Phys. **22**, 19 (1977)